
Incremental Neural Implicit Representation with Uncertainty-Filtered Knowledge Distillation

Mengqi Guo* Chen Li* Hanlin Chen Gim Hee Lee

Department of Computer Science, National University of Singapore
{mengqi, lic, hanlin.chen, gimhee.lee}@comp.nus.edu.sg

Abstract

Recent neural implicit representations (NIRs) have achieved great success in the tasks of 3D reconstruction and novel view synthesis. However, they suffer from the catastrophic forgetting problem when continuously learning from streaming data without revisiting the previously seen data. This limitation prohibits the application of existing NIRs to scenarios where images come in sequentially. In view of this, we explore the task of incremental learning for NIRs in this work. We design a student-teacher framework to mitigate the catastrophic forgetting problem. Specifically, we iterate the process of using the student as the teacher at the end of each time step and let the teacher guide the training of the student in the next step. As a result, the student network is able to learn new information from the streaming data and retain old knowledge from the teacher network simultaneously. Although intuitive, naively applying the student-teacher pipeline does not work well in our task. Not all information from the teacher network is helpful since it is only trained with the old data. To alleviate this problem, we further introduce a random inquirer and an uncertainty-based filter to filter useful information. Our proposed method is general and thus can be adapted to different implicit representations such as neural radiance field (NeRF) and neural SDF. Extensive experimental results for both 3D reconstruction and novel view synthesis demonstrate the effectiveness of our approach compared to different baselines.

1 Introduction

Recent neural implicit representations (NIRs) [28, 44, 49, 53] such as NeRF and neural SDF have attracted increasing attention in the last few years because of their great success in novel view synthesis and 3D reconstruction. The key to these representations is to memorize the volume density or SDF value and view-dependent color of every spatial point in the scene with a multi-layer perceptron (MLP). Although the simple MLP networks implicitly represent the 3D scenes precisely, they require images of a scene at different camera views to be available for a one-time training. This is not applicable to real-world scenarios where streaming data comes in sequentially or where only limited data storage is available. In view of this limitation, we explore an important task of incremental learning for NIRs in this work. In the incremental setting, the model trains on the current data without accessing any previous data, but tests on both current and previous data.

The main challenge for incremental learning is the catastrophic forgetting problem [33], where the network trained on only new incoming images drastically forgets the previously learned knowledge. This is evident from the result of MonoSDF [53] in Fig. 1, where the network is trained continuously with new incoming data captured along the yellow trajectory. The triangles represent camera views at different time steps, and green denotes camera view at current time step and gray ones for previous steps. We can see that the model fails to reconstruct the 3D scene observed at $t = 0$ after being

*Equal contribution

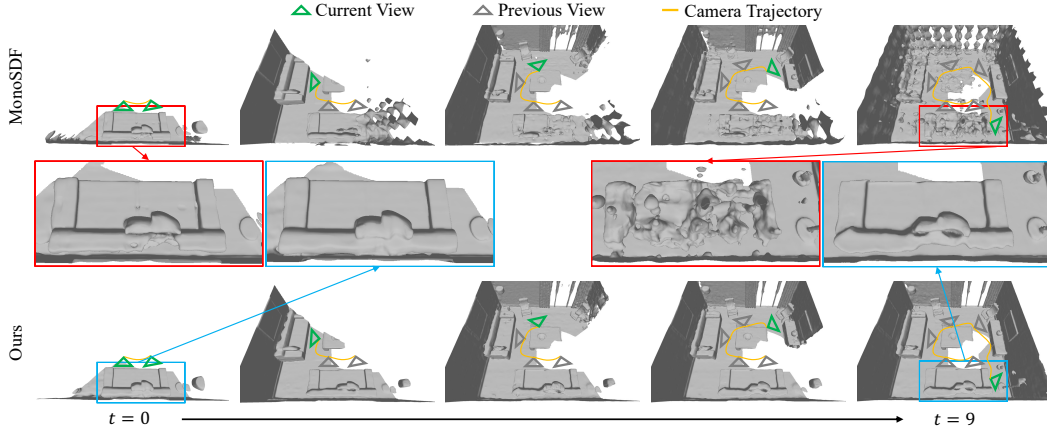


Figure 1: Visualization of the 3D reconstruction by MonoSDF [53] and our approach under the incremental setting. MonoSDF fails to reconstruct 3D surface observed at $t = 0$ after being trained with new data because of the forgetting problem. In comparison, our approach is able to reconstruct both previously seen and new data.

trained with new data. The catastrophic forgetting problem is widely discussed in the incremental learning literature [2, 25, 1, 56, 21], and the most related work to ours is Continual Neural Mapping (CNM) [48]. CNM is the first work that introduces the incremental setting for 3D reconstruction using Signed Distance Function (SDF). A data-replay strategy [19] is adopted in CNM to mitigate the forgetting problem. However, the data-replay still requires part of the previous training data to be stored. Additionally, CNM only shows results for SDF-based 3D reconstruction, while we aim for a general pipeline for different NIRs such as NeRF and Neural SDF.

In this work, we propose a student-teacher pipeline to tackle the catastrophic forgetting problem in the incremental NIRs. Specifically, we first train the model with the currently available data, and then use the trained model as the teacher model to generate supervision for the student model. We iterate this process by using the student as the teacher at the end of each time step, and letting the teacher guide the training of the student in the next step. As a result, the student network is able to learn from the newly available data and preserves the old knowledge from the teacher network simultaneously. Furthermore, we also propose an alternate optimization strategy such that the new data and knowledge from the teacher network can be effectively imparted to the student network.

The aim of introducing the teacher network is to impart the knowledge obtained from the previous training steps to the current student network. However, the teacher network which has only been trained with the old data is unable to generate useful knowledge for the unseen data. To solve this problem, we further introduce a random inquirer and an uncertainty-based filter for filtering useful knowledge. The inquirer randomly generates camera views for the uncertainty module and the filter removes the uncertain queries based on a confidence score. Intuitively, the uncertainty module would only have high confidence for the previously seen or similar data, and hence it is able to filter out the incorrect knowledge generated from the random query.

We evaluate the effectiveness of our proposed approach on two popular NIRs, NeRF and neural SDF. Extensive experimental results on both 3D reconstruction and novel view synthesis show that our approach mitigates the catastrophic forgetting problems effectively without storing previous training data. Specifically, our method significantly improves 39.6% and 61.3% over MonoSDF in terms of F1 on the ICL-NUIM and Replica datasets. Moreover, our approach outperforms NeRF by 36.3% and 63.9% in terms of PSNR on the NeRF-real360 and ScanNet datasets, respectively. Our contributions are summarized as follows:

- We explore the task of incremental learning for general neural implicit representations.
- We propose a student-teacher pipeline to mitigate catastrophic forgetting in incremental learning.
- We design the uncertainty filter and the random inquirer to generate and select useful information for the student network.

- We significantly outperform baselines by a large margin for both 3D reconstruction and novel view synthesis.

2 Related Work

Neural Implicit Representation. The neural implicit representations (NIRs) have shown remarkable potential in various computer vision tasks, such as novel view synthesis [28, 4, 5] and 3D reconstruction [44, 49, 53, 3, 42], depth estimation [20, 46], and camera pose estimation [50, 22]. The pioneering work NeRF [28] introduced a simple yet effective multi-layer perceptron (MLP) network to implicitly capture the 3D scene and propose a differentiable rendering method for generating novel view images. Many follow-up works have attempted to enhance NIRs to fully exploit their potential, such as real-time rendering [51, 32], faster training [23, 12, 29, 7], sparse view input [52, 34], generalizable model [45, 8], scalable model [55, 43], lightning changing [26, 27], robust training [22], better representation [4, 54], *etc.* Some recent works [44, 49] proposed neural implicit surfaces and incorporated the signed distance function (SDF) into NeRF for smooth and accurate surface reconstruction. MonoSDF [53] further leveraged monocular prior to achieve more detailed reconstruction for larger 3D scenes. Despite the great success, existing NIRs suffer from the catastrophic forgetting problem when continuously learning from streaming data. In view of this, we focus on the under-explored and yet important incremental settings for NIRs in this paper.

Incremental Learning. Incremental learning is a classical machine learning problem where only partial data is available for training at each step. Existing methods typically fall into three categories [10]: data replay [17, 31, 35, 24, 6, 39], parameter regularization [21, 30, 1, 16], and parameter isolation [2, 47, 25, 11]. In this paper, we revisit some classical incremental approaches to build strong baselines. Specifically, PTAM [17] introduced a set of keyframes as a long-term scene representation and replayed them to avoid forgetting, MAS [1] measured the parameter importance for each task and regularized the important parameters to preserve previously learned knowledge, while PackNet [25] assigned parameters subsets explicitly to different tasks by constituting binary masks. Continual Neural Mapping (CNM) [48] is the first work on incremental learning for neural SDF, which reconstructs 3D surface from streaming depth inputs using a replay-based method [19]. However, their method still requires access to some of the previous data to prevent forgetting and they mainly focus on the SDF representation. In comparison, our approach can be adapted to different NIRs without access to any previous data.

NIR-SLAM and Large-scale NeRF. Traditional simultaneous localization and mapping (SLAM) is able to reconstruct 3D scenes with streaming data, which share similar spirits with our incremental setting. Recently, some works such as iMAP [41], NICE-SLAM [57], and NeRF-SLAM [36] adopt neural implicit representation as the scene representation in SLAM and achieve promising performance. These approaches mitigate the forgetting problem by storing keyframes, as done in traditional SLAM. The drawback of using keyframes is that memory usage will increase accordingly as the scene gets larger. On the other hand, Recent NeRFusion [55] and Block-NeRF [43] handle large-scale scenes by incrementally reconstructing a global scene representation by fusing local voxel representations. However, the voxel-based representation requires substantial storage and the fusion stage requires all the images of a scene. Moreover, all those approaches work on one specific neural implicit representation while we propose a general approach, which is also memory-efficient.

3 Preliminaries: Neural Implicit Representations

In this section, we present a unified formulation for the currently dominant NIRs including NeRF [28] and neural SDF [49, 53]. The principal idea is to use a simple neural network such as MLPs to memorize the color $\mathbf{c} = (r, g, b)$, volume density σ for each location $\mathbf{x} = (x, y, z)$ and camera view direction $\mathbf{d} = (\theta, \phi)$ in a 3D scene. While existing neural SDF predicts SDF value which is then converted to density, we use $(\mathbf{c}, \sigma) = F(\mathbf{x}, \mathbf{d})$ to represent both NeRF and neural SDF networks in this paper for simplicity. The per-pixel RGB $c(\mathbf{r})$ value of an image can be rendered with N 3D points taken along the ray \mathbf{r} from the camera center to the pixel as:

$$c(\mathbf{r}) = \sum_{i=1}^N T_i (1 - \exp(-\sigma_i \delta_i)) \mathbf{c}_i, \quad T_i = \exp\left(-\sum_{j=1}^{i-1} \sigma_j \delta_j\right), \quad (1)$$

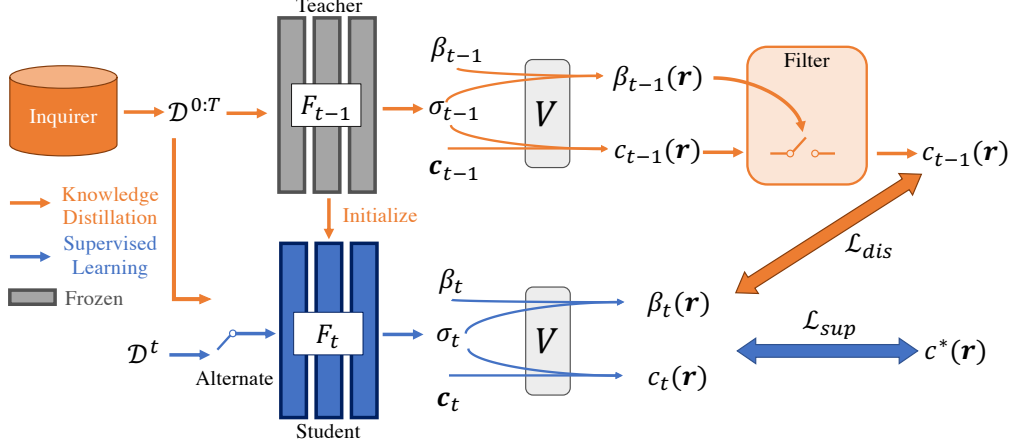


Figure 2: The overall framework of our proposed student-teacher pipeline. At time step t , The student network learns simultaneously from the currently available data \mathcal{D}^t and the previously learned knowledge from the teacher network. The input of the teacher network is generated with the random inquirer. The output is filtered with an uncertainty based filter for useful information selection. V denotes the differentiable volume renderer.

where δ_i indicates the distance between i^{th} sample and $(i + 1)^{\text{th}}$ sample, and T_i is the accumulated transmittance along the ray \mathbf{r} from camera center to i^{th} 3D point. Since the whole pipeline is differentiable, the rendering output can be directly supervised by the RGB image with the L2 distance:

$$\mathcal{L} = \mathcal{L}_{rgb} + [\mathcal{L}_{eikonal}] + [\mathcal{L}_{prior}], \quad \mathcal{L}_{rgb} = \sum_{\mathbf{r} \in R} \left(\|c^*(\mathbf{r}) - c(\mathbf{r})\|_2^2 \right), \quad (2)$$

where $c^*(\mathbf{r})$ denotes the ground truth color, R represents a group of rays from one or more camera views, \mathcal{L}_{rgb} represents the rendering loss, $\mathcal{L}_{eikonal}$ the SDF regularizer for neural SDF [44, 49, 53], and \mathcal{L}_{prior} the optional geometry prior [53]. Note that \mathcal{L}_{rgb} is the fundamental term for both NeRF and neural SDF and $\mathcal{L}_{eikonal}$ or \mathcal{L}_{prior} extra regularizer or prior terms used in existing works, which we denote with $[\cdot]$.

3.1 Catastrophic Forgetting of NIRs

Despite the impressive performance, existing NIRs require training on the entire set of images covering all views. In practice, this may not be feasible in the scenario of limited data storage or streaming data, which may require the network to be trained on new data without revisiting old ones. This may lead to the catastrophic forgetting of existing NIRs, where the network quickly forgets previously learned knowledge while acquiring new knowledge. To address this issue, we explore the task of incremental learning for NIRs with the goal of mitigating the catastrophic forgetting problem.

4 Our Method

In this section, we first introduce the incremental setting for NIRs. We then represent our proposed student-teacher pipeline with an uncertainty based filter and an alternative optimization strategy.

4.1 Problem Definition

We consider a common scenario in the robotics or vision community, where $T + 1$ groups of data $\mathcal{D} = \{\mathcal{D}^0, \mathcal{D}^1, \dots, \mathcal{D}^T\}$ come in sequentially. The data for each time step t consists of N pairs of images I^t and the corresponding camera poses P^t , i.e., $\mathcal{D}^t = \{d_0^t, d_1^t, \dots, d_N^t\}$, where $d_n^t = (I_n^t, P_n^t)$. Generally, the camera poses do not overlap between different time steps $P^i \cap P^j = \emptyset, \forall i, j \in \{0, 1, \dots, T\}, i \neq j$. The task of incremental learning for NIRs aims to continually learn from the newly arriving data \mathcal{D}^t and also preserve the knowledge from previously seen data $\mathcal{D}^{0:t-1}$.

4.2 Overview

The overall framework of our approach is illustrated in Fig. 2. It comprises a student and a teacher network, both sharing the same architecture with a density branch, a color branch, and an uncertainty branch. At each time step t , the student learns simultaneously from the currently available data \mathcal{D}^t and the previously learned knowledge from the teacher network. The student model trained in this step is then utilized as the teacher model in the next step and imparts its acquired knowledge to the next student. We iterate this process throughout the training process. To explore the knowledge space of the teacher network, we design a random inquirer that generates camera views for the teacher network. However, the teacher network can generate erroneous information for randomly generated views because it only trains on previously seen data $\mathcal{D}^{0:t-1}$. We further design an uncertainty branch to predict uncertainty score and select only reliable information from the teacher network.

4.3 Supervised Learning

At each time step t , we utilize the available data \mathcal{D}^t to train the student network directly with rendering loss. Except for the density and color, we also predict the uncertainty value for each input to measure the confidence.

Uncertainty Modeling. We adopt the self-supervised uncertainty formulation from [15] to model the uncertainty of the network for each input ray. This formulation has also been used in previous NeRF-in-the-Wild [26] to distinguish the static and transient scenes. With a different objective, we aim to utilize the uncertainty output to indicate the confidence of the network on the current input. Specifically, we build an additional branch that shares the same input as the color branch to predict the uncertainty $(\mathbf{c}, \sigma, \beta) = F(\mathbf{x}, \mathbf{d})$. We adopt Softplus as the activation function on the uncertainty for stable training. Finally, we compute the pixel-wise uncertainty from each sample point using the same volume rendering technique as the color:

$$\beta(\mathbf{r}) = \sum_{n=1}^N T_i (1 - \exp(-\sigma_j \delta_j)) \hat{\beta}_i + \beta_{min}, \quad \hat{\beta}_i = \log(1 + e^{\beta_i - 1}), \quad (3)$$

where T_i represents the accumulated transmittance expressed by Eqn. (1), and β_{min} denotes a hyper-parameter that ensures the minimum uncertainty following [26].

Supervised Optimization. The objective function of the supervised training is expressed as:

$$\mathcal{L}_{sup} = \sum_{\mathbf{r} \in R} \left(\frac{\|c^*(\mathbf{r}) - c_t(\mathbf{r})\|_2^2}{2} + \frac{\|c^*(\mathbf{r}) - c_t(\mathbf{r})\|_2^2}{2 * \beta_t(\mathbf{r})^2} + \log(\beta_t(\mathbf{r})) + \eta \right), \quad (4)$$

where η denotes the margin of the uncertainty regular term to avoid negative values. Note that we only need to supervise the color and the uncertainty is implicitly learned from the loss function. Intuitively, on one hand, the network needs to predict a high uncertainty value when the color prediction is inaccurate in order to minimize the loss function. On the other hand, the regularization term $\log(\beta_t(\mathbf{r}))$ prevents the network from predicting infinite uncertainty.

4.4 Knowledge Distillation

The network trained with only the currently available data at each time step tends to forget the previously learned knowledge, referred as the catastrophic forgetting problem. To prevent this, we further introduce a teacher network to impart the previously learned knowledge to the current model.

Student-teacher Modeling. At each time step t , the student network F_t concurrently learns from the teacher network F_{t-1} and the new coming data \mathcal{D}^t . The student network is then used as the teacher network after each step. We iterate the process of using the student as the teacher at the end of each step, and let the teacher guide the student in the next step. As a result, the student network can learn both new knowledge from the new data and old knowledge from the teacher network and hence mitigating the forgetting problem. To facilitate the knowledge imparting from the teacher to the student network, we introduce a knowledge distillation loss [14]. Moreover, we initialize the parameters of the student network with that of the teacher network. This initialization strategy also helps to mitigate the forgetting problem since the parameters are learned from previously seen data.

Random Inquirer. The role of the teacher network is to impart old knowledge, which means the inputs should be the same as the training data from the previous time steps. However, the previous training data is not accessible under the incremental setting. To solve this problem, we design a constrained random inquirer to generate inputs for the teacher network. The randomly generated inputs should fulfill some constraints specific to different types of datasets, which we explain in more detail in the supplementary material.

Uncertainty-based Filter. The role of the random inquirer is to explore the knowledge space of the teacher network such that we can extract useful information, *i.e.* the knowledge from previous time steps. However, the teacher network might output incorrect knowledge since it has been trained only on $D^{0:t-1}$, while the input generated from the random inquirer covers the whole dataset. To overcome this issue, we utilize the uncertainty module as described in Sec. 4.3 for useful knowledge selection. Specifically, we take the average of the output uncertainty value over rays from one camera view, and only select camera views with an uncertainty smaller than a threshold β^{thr} , *i.e.*:

$$R^* \leftarrow R^* \cup R_v, \quad \text{if } \frac{1}{\mathcal{N}_{R_v}} \sum_{\mathbf{r} \in R_v} (\beta_t(\mathbf{r})) < \beta^{thr}, \quad (5)$$

where R_v is the rays for camera view v generated from the random inquirer, \mathcal{N}_{R_v} is the number of rays samples, and R^* is the collection of data samples we use for knowledge distillation. Intuitively, the network tends to output lower uncertainty for previously seen data compared to unseen ones, and thus we can use R^* to approximate the unavailable data from the previous training step. Note that the selection is conducted in terms of camera views, *i.e.* average over all ray samples instead of a single ray. This is empirically shown to better distinguish the seen and unseen images.

Distilled Optimization. Finally, we use the teacher network to guide the student network via a knowledge distillation loss:

$$\mathcal{L}_{dis} = \sum_{\mathbf{r} \in R^*} \left(\frac{\|c_{t-1}(\mathbf{r}) - c_t(\mathbf{r})\|_2^2}{2} + \frac{\|c_{t-1}(\mathbf{r}) - c_t(\mathbf{r})\|_2^2}{2 * \beta_t(\mathbf{r})^2} + \log(\beta_t(\mathbf{r})) + \eta \right), \quad (6)$$

where $c_{t-1}(\mathbf{r})$ and $c_t(\mathbf{r})$ represent the output color of the teacher and student model, respectively. R^* denotes useful data selection from Eqn. (5). With knowledge distillation, the student network is able to preserve the previously learned knowledge throughout the whole training process.

4.5 Iterative Optimization

We propose an iterative optimization mechanism to enable the student network to learn simultaneously from the current data \mathcal{D}^t and knowledge from the teacher network. Specifically, we alternatively optimize the supervised loss Eqn. (4) and the knowledge distillation loss Eqn. (6), *i.e.*:

$$\mathcal{L} = \begin{cases} \mathcal{L}_{sup} + [\mathcal{L}_{eikonal}] + [\mathcal{L}_{prior}], & \text{if } i \% 2 == 0 \\ \mathcal{L}_{dis} + [\mathcal{L}_{eikonal}] + [\mathcal{L}_{prior_dis}], & \text{otherwise} \end{cases}, \quad (7)$$

where i denotes the iteration number, \mathcal{L}_{prior_dis} represents that the prior comes from the teacher network instead of the pre-trained model as in the \mathcal{L}_{prior} .

5 Experiments

5.1 Experimental Settings

We apply our approach to the currently dominant implicit representations NeRF [28] and neural SDF [53], and show results for both novel view synthesis and 3D reconstruction.

Dataset. The previous NIRs conducted experiments on different types of scenes, thus we consider the following datasets to cover these types: a) Object-centric scenes: NeRF-real360 [28]; b) Room-scale synthetic scans: ICL-NUIM [13] and Replica [40]; c) Room-scale real-world scans: ScanNet [9]. For incremental setting, we divide the images of each scene and the corresponding camera poses into 10 time steps $\mathcal{D} = \{\mathcal{D}^0, \mathcal{D}^1, \dots, \mathcal{D}^9\}$.

Baselines. We compare against a) the original NeRF [28] and MonoSDF [53] under both incremental and batch training settings; b) SLAM-based NIRs iMAP [41] and NICE-SLAM [57]; c) Reply-based incremental neural SDF method CNM [48]; d) Three most representative baselines for incremental learning MAS [1], PackNet [25], KeyF [17] (implemented with 10 keyframes following iMAP [41]).

Evaluation Metrics. For 3D reconstruction, we report Chamfer Distance (CD) and F1 score with a threshold of 5cm, following MonoSDF [53]. For novel view synthesis, we report PSNR, SSIM, and LPIPS following NeRF [28].

Table 1: Comparison with baselines on the ICL-NUIM dataset. (Best and second best results are highlighted in bold and underlined, respectively.)

	MonoSDF [53]	MonoSDF* [53]	CNM [48]	MAS [1]	PackNet [25]	KeyF [17]	Ours
F1↑	64.71	89.68	-	66.40	76.03	<u>86.78</u>	90.32
CD↓	5.94	2.64	5.42	5.84	4.39	<u>3.02</u>	2.60

Table 2: Comparison with baselines on the replica dataset. (Best and second best results are highlighted in bold and underlined, respectively.)

	MonoSDF [53]	MonoSDF* [53]	iMAP [41]	NICE-SLAM [57]	MAS [1]	PackNet [25]	KeyF [17]	Ours
F1↑	53.63	86.18	-	-	58.75	61.99	<u>79.67</u>	86.52
CD↓	8.58	2.94	4.99	2.93	7.98	7.49	3.99	<u>3.11</u>

5.2 Results on 3D Reconstruction

We first evaluate our approach for the neural SDF based representation. We adopt MonoSDF as the backbone and show 3D reconstruction results on the ICL-NUIM and Replica datasets.

ICL-NUIM. We show the results of our approach and the baselines on the ICL-NUIM dataset in Tab. 1. We can see that the performance of MonoSDF drops significantly when trained under incremental setting compared to the results under batch training (MonoSDF*). Note that batch training means that all data are available for one-time training, which is the upper bound of incremental training. The incremental baselines only achieve minor improvement compared with MonoSDF with the exception of KeyF. However, KeyF requires more memory as will described in Section 5.6. In comparison, our approach improves over the MonoSDF baseline by 39.6% in F1 and is even slightly better than batch training while keeping a low memory usage.

Replica. We further show results on the Replica dataset in Tab. 2. We can see that MonoSDF and incremental baselines (MAS, PackNet, and KeyF) suffer from the forgetting problem, which can be evident from the performance drop compared to MonoSDF*. Our approach improves MonoSDF by 61.3% for F1 and also achieves similar performance with batch training. Compared to the SLAM-based baselines, our model outperforms iMAP by a large margin and is only slightly worse than NICE-SLAM. The better performance of NICE-SLAM can be attributed to the use of more powerful representations compared to our backbone MonoSDF. Moreover, the memory usage of SLAM-based baselines increase as the scene gets larger. Note that we compare with different baselines on the two datasets since CNM and SLAM-based NIRs (iMAP, NICE-SLAM) show results on the ICL-NUIM and Replica, respectively.

Table 3: Quantitative comparison with baselines on the NeRF-real360 dataset. We show results for each step test datasets \mathcal{D}^0 , \mathcal{D}^3 , \mathcal{D}^6 , \mathcal{D}^9 and the average performance over $\mathcal{D}^{0:9}$, respectively.

Method	Test Dataset (PSNR↑ / SSIM↑ / LPIPS↓)				Average on $\mathcal{D}^{0:9}$
	\mathcal{D}^0	\mathcal{D}^3	\mathcal{D}^6	\mathcal{D}^9	
NeRF [28]	16.10 / 0.468 / 0.276	14.97 / 0.407 / 0.357	15.50 / 0.512 / 0.323	18.18 / 0.636 / 0.217	15.56 / 0.468 / 0.317
NeRF* [28]	24.27 / 0.781 / 0.177	23.81 / 0.767 / 0.184	22.86 / 0.738 / 0.188	20.75 / 0.684 / 0.227	22.81 / 0.741 / 0.198
MAS [1]	18.15 / 0.552 / 0.273	16.42 / 0.500 / 0.332	16.95 / 0.525 / 0.374	17.35 / 0.551 / 0.340	17.02 / 0.513 / 0.341
PackNet [25]	17.21 / 0.497 / 0.349	17.09 / 0.491 / 0.378	17.01 / 0.489 / 0.390	14.45 / 0.417 / 0.447	16.52 / 0.474 / 0.388
KeyF [17]	18.76 / 0.629 / 0.225	19.50 / 0.625 / 0.238	21.14 / 0.682 / 0.213	19.46 / 0.657 / 0.328	19.68 / 0.642 / 0.240
Ours	22.48 / 0.701 / 0.188	22.16 / 0.694 / 0.208	21.07 / 0.682 / 0.173	19.82 / 0.658 / 0.221	21.21 / 0.672 / 0.211

5.3 Results on Novel View Synthesis

We then evaluate our approach for neural radiance field based representation. We adopt NeRF as our backbone and show results for the NeRF-real360 and ScanNet datasets. The four columns \mathcal{D}^0 , \mathcal{D}^3 , \mathcal{D}^6 , \mathcal{D}^9 denote the testing dataset at the corresponding time step. The results are obtained from the final model, which has been trained incrementally on all views $\mathcal{D}^{0:9}$.

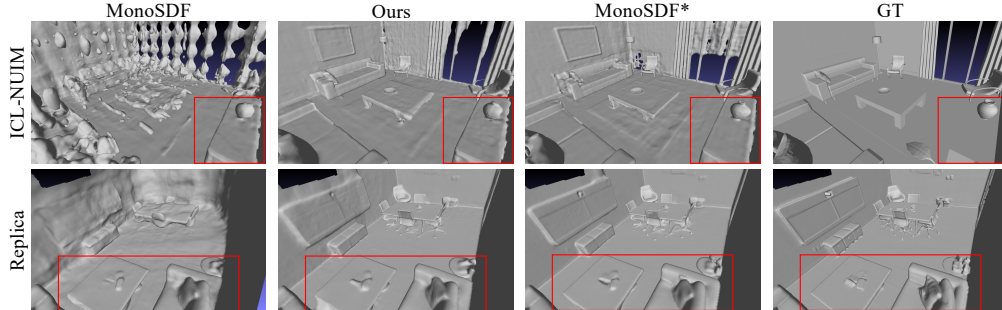


Figure 3: Qualitative comparison on the ICL-NUIM and Replica datasets. Both ‘MonoSDF’ and ‘Ours’ models are incrementally trained on the 10-step training datasets. The red boxes denote current views, and the rest are the previous views.

NeRF-real360. We show the results of our approach and baselines on the NeRF-real360 [28] dataset in Tab. 3. We can see that the NeRF baseline suffers from the forgetting problem, leading to a large performance drop on the testing data at previous steps $\mathcal{D}^0, \mathcal{D}^3, \mathcal{D}^6$. The incremental baselines (MAS, PackNet, and KeyF) mitigate the forgetting problem to some extent with limited improvement. In comparison, our approach is able to perform consistently well on previous testing data with improvements over the NeRF baseline by 39.6%, 48.0%, and 35.9% for $\mathcal{D}^0, \mathcal{D}^3, \mathcal{D}^6$, and 36.3% for $\mathcal{D}^{0:9}$ in PSNR.

ScanNet. We further show results for the more challenging large-scale ScanNet [9] dataset in Tab. 4. We can see that both the NeRF baseline and incremental baselines perform poorly on the testing datasets of previous time steps because of the severe forgetting problem caused by little overlap between images in this dataset. Benefiting from the student-teacher pipeline, our method still achieves promising results with significant improvements over incremental baselines (MAS, PackNet, and KeyF) and SLAM-based baseline iMAP. Comparable performance is also achieved with batch training NeRF*, which further demonstrates the effectiveness of our approach.

Table 4: Quantitative comparison with baselines on the ScanNet dataset. We show results for each step test datasets $\mathcal{D}^0, \mathcal{D}^3, \mathcal{D}^6, \mathcal{D}^9$ and the average performance over $\mathcal{D}^{0:9}$, respectively.

Method	Test Dataset (PSNR↑ / SSIM↑ / LPIPS↓)				Average on $\mathcal{D}^{0:9}$
	\mathcal{D}^0	\mathcal{D}^3	\mathcal{D}^6	\mathcal{D}^9	
NeRF [28]	12.61 / 0.580 / 0.396	11.59 / 0.505 / 0.571	15.65 / 0.578 / 0.470	25.95 / 0.876 / 0.145	13.78 / 0.576 / 0.460
NeRF* [28]	22.55 / 0.824 / 0.244	22.23 / 0.850 / 0.231	24.53 / 0.860 / 0.211	25.51 / 0.881 / 0.150	23.55 / 0.852 / 0.212
iMAP [41]	10.85 / 0.581 / 0.472	19.53 / 0.808 / 0.300	19.19 / 0.789 / 0.326	20.88 / 0.794 / 0.328	18.80 / 0.761 / 0.340
MAS [1]	16.40 / 0.669 / 0.366	12.15 / 0.595 / 0.512	15.76 / 0.684 / 0.455	22.22 / 0.812 / 0.303	15.76 / 0.673 / 0.402
PackNet [25]	12.74 / 0.535 / 0.488	11.99 / 0.604 / 0.456	13.60 / 0.630 / 0.429	11.49 / 0.550 / 0.457	12.75 / 0.592 / 0.439
KeyF [17]	14.03 / 0.598 / 0.392	12.72 / 0.583 / 0.525	16.69 / 0.691 / 0.396	22.02 / 0.801 / 0.271	16.04 / 0.663 / 0.397
Ours	21.74 / 0.812 / 0.224	20.21 / 0.825 / 0.296	23.90 / 0.851 / 0.224	25.30 / 0.876 / 0.162	22.59 / 0.841 / 0.230

5.4 Ablation Study

As shown in Tab. 5, we conduct ablation studies for both neural SDF and NeRF representations on the ICL-NUIM and NeRF-real360 datasets, respectively. We verify the contribution of our proposed components student-teacher modeling (s-t) and uncertainty-based filter (filter) by removing each component at a time. As can be seen that the performance drops when each component is removed. Specifically, our approach becomes the original NeRF or MonoSDF when the student-teacher modeling is removed, and the model fails completely. Without the uncertainty-based filter, the performance drops significantly for incremental 3D reconstruction task on the ICL-NUIM dataset. This is because the output of the teacher network is not necessarily correct for any input generated from the random inquirer, and the incorrect information can mislead the student during the knowledge distillation. Additionally, we also show results when the camera poses of previous time steps are stored, denoted as w/ $P^{0:t}$. We can see that we achieve comparable performance with this scenario although we do not store any data from previous time step.

Table 5: Ablation studies on ICL-NUIM and NeRF-real360.

Method	ICL-NUIM		NeRF-real360
	F1↑	CD↓	PSNR↑
w/o s-t	64.71	5.94	15.56
w/o filter	81.63	3.82	19.39
Ours	90.32	2.60	21.21
w/ $P^{0:t}$	89.50	2.65	21.38

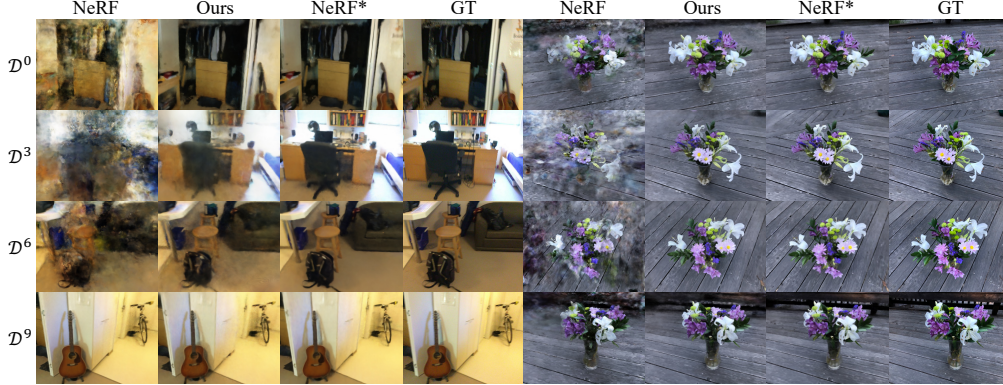


Figure 4: Qualitative comparison on the ScanNet and NeRF-real360 datasets. $\mathcal{D}^0, \mathcal{D}^3, \mathcal{D}^6, \mathcal{D}^9$ denote the results from each time step test views. ‘NeRF’ and ‘Ours’ models are incrementally trained on the 10-step training datasets.

5.5 Visualization

3D Reconstruction. We show the qualitative comparison of the ICL-NUIM and Replica datasets in Fig. 3. We can see that MonoSDF baseline learns well for the current scene (highlight with red boxes) but fails on previously seen scenes (scenes outside the red box) completely. In comparison, our approach is able to reconstruct detailed geometries for both current and previous scenes, achieving similar quality with “MonoSDF*” and ground truth.

Novel View Synthesis. We show qualitative comparison on the ScanNet scene 101 and NeRF-real360 scene *Vasdeck* in Fig. 4. As we can see, the original NeRF suffers from the catastrophic forgetting problem and outputs images on previous time steps $\mathcal{D}^0, \mathcal{D}^3, \mathcal{D}^6$ with severe artifacts including noise and blur. In comparison, our approach generates realistic images with comparable quality to the batch training. This suggests the effectiveness of our proposed approach in mitigating the forgetting problem.

5.6 Memory Analysis

Keyframe-based technique plays a crucial role in mitigating the forgetting problem in existing SLAM-based methods [41, 57] and incremental NIRs [48]. These approaches require additional memory allocation to store the previously seen data. To understand the relationship between memory utilization and performance, we conducted experiments using the KeyF baseline with varying memory capacities, as shown in Fig. 5. We can see that performance improves as memory usage increases from 0 (equivalent to MonoSDF baseline) to 270MB (equivalent to batch training). In comparison, our approach outperforms similar to batch training while maintaining minimal memory consumption.

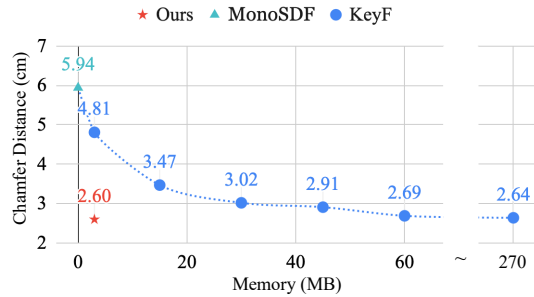


Figure 5: Memory analysis on ICL-NUIM.

6 Conclusion

In this paper, we explore the task of incremental learning for Neural Implicit Representations (NIRs). We propose a student-teacher pipeline for mitigating the catastrophic forgetting problem. To improve the effectiveness of the data provided by the teacher network, we further design a random inquirer and an uncertainty-based filter for useful knowledge distillation. Experiments on both 3D reconstruction and novel view synthesis demonstrate that our model achieves great improvement compared to baselines under the incremental setting.

References

- [1] Rahaf Aljundi, Francesca Babiloni, Mohamed Elhoseiny, Marcus Rohrbach, and Tinne Tuytelaars. Memory aware synapses: Learning what (not) to forget. In *ECCV*, 2018.
- [2] Rahaf Aljundi, Punarjay Chakravarty, and Tinne Tuytelaars. Expert gate: Lifelong learning with a network of experts. In *CVPR*, 2017.
- [3] Dejan Azinović, Ricardo Martin-Brualla, Dan B Goldman, Matthias Nießner, and Justus Thies. Neural rgb-d surface reconstruction. In *CVPR*, 2022.
- [4] Jonathan T Barron, Ben Mildenhall, Matthew Tancik, Peter Hedman, Ricardo Martin-Brualla, and Pratul P Srinivasan. Mip-nerf: A multiscale representation for anti-aliasing neural radiance fields. In *ICCV*, 2021.
- [5] Jonathan T Barron, Ben Mildenhall, Dor Verbin, Pratul P Srinivasan, and Peter Hedman. Mip-nerf 360: Unbounded anti-aliased neural radiance fields. In *CVPR*, 2022.
- [6] Arslan Chaudhry, Marc’ Aurelio Ranzato, Marcus Rohrbach, and Mohamed Elhoseiny. Efficient lifelong learning with a-gem. *arXiv preprint arXiv:1812.00420*, 2018.
- [7] Anpei Chen, Zexiang Xu, Andreas Geiger, Jingyi Yu, and Hao Su. Tensorf: Tensorial radiance fields. *ECCV*, 2022.
- [8] Anpei Chen, Zexiang Xu, Fuqiang Zhao, Xiaoshuai Zhang, Fanbo Xiang, Jingyi Yu, and Hao Su. Mvsnerf: Fast generalizable radiance field reconstruction from multi-view stereo. In *ICCV*, 2021.
- [9] Angela Dai, Angel X. Chang, Manolis Savva, Maciej Halber, Thomas Funkhouser, and Matthias Nießner. Scannet: Richly-annotated 3d reconstructions of indoor scenes. In *CVPR*, 2017.
- [10] Matthias De Lange, Rahaf Aljundi, Marc Masana, Sarah Parisot, Xu Jia, Aleš Leonardis, Gregory Slabaugh, and Tinne Tuytelaars. A continual learning survey: Defying forgetting in classification tasks. *TPAMI*, 2021.
- [11] Chrisantha Fernando, Dylan Banarse, Charles Blundell, Yori Zwols, David Ha, Andrei A Rusu, Alexander Pritzel, and Daan Wierstra. Pathnet: Evolution channels gradient descent in super neural networks. *arXiv preprint arXiv:1701.08734*, 2017.
- [12] Sara Fridovich-Keil, Alex Yu, Matthew Tancik, Qinhong Chen, Benjamin Recht, and Angjoo Kanazawa. Plenoxels: Radiance fields without neural networks. In *CVPR*, 2022.
- [13] A. Handa, T. Whelan, J.B. McDonald, and A.J. Davison. A benchmark for RGB-D visual odometry, 3D reconstruction and SLAM. In *ICRA*, 2014.
- [14] Geoffrey Hinton, Oriol Vinyals, Jeff Dean, et al. Distilling the knowledge in a neural network. *arXiv preprint arXiv:1503.02531*, 2015.
- [15] Alex Kendall and Yarin Gal. What uncertainties do we need in bayesian deep learning for computer vision? *NeurIPS*, 2017.
- [16] James Kirkpatrick, Razvan Pascanu, Neil Rabinowitz, Joel Veness, Guillaume Desjardins, Andrei A Rusu, Kieran Milan, John Quan, Tiago Ramalho, Agnieszka Grabska-Barwinska, et al. Overcoming catastrophic forgetting in neural networks. *Proceedings of the national academy of sciences*, 2017.
- [17] Georg Klein and David Murray. Parallel tracking and mapping for small ar workspaces. In *ISMAR*, 2007.
- [18] Alex Krizhevsky, Ilya Sutskever, and Geoffrey E Hinton. Imagenet classification with deep convolutional neural networks. *Communications of the ACM*, 2017.
- [19] Soochan Lee, Junsoo Ha, Dongsu Zhang, and Gunhee Kim. A neural dirichlet process mixture model for task-free continual learning. *ICLR*, 2020.
- [20] Jiaxin Li, Zijian Feng, Qi She, Henghui Ding, Changhu Wang, and Gim Hee Lee. Mine: Towards continuous depth mpi with nerf for novel view synthesis. In *CVPR*, 2021.
- [21] Zhizhong Li and Derek Hoiem. Learning without forgetting. *TPAMI*, 2017.
- [22] Chen-Hsuan Lin, Wei-Chiu Ma, Antonio Torralba, and Simon Lucey. Barf: Bundle-adjusting neural radiance fields. In *ICCV*, 2021.
- [23] Lingjie Liu, Jiatao Gu, Kyaw Zaw Lin, Tat-Seng Chua, and Christian Theobalt. Neural sparse voxel fields. *NeurIPS*, 2020.
- [24] David Lopez-Paz and Marc’ Aurelio Ranzato. Gradient episodic memory for continual learning. *NeurIPS*, 2017.
- [25] Arun Mallya and Svetlana Lazebnik. Packnet: Adding multiple tasks to a single network by iterative pruning. In *CVPR*, 2018.
- [26] Ricardo Martin-Brualla, Noha Radwan, Mehdi SM Sajjadi, Jonathan T Barron, Alexey Dosovitskiy, and Daniel Duckworth. Nerf in the wild: Neural radiance fields for unconstrained photo collections. In *CVPR*, 2021.

- [27] Ben Mildenhall, Peter Hedman, Ricardo Martin-Brualla, Pratul P Srinivasan, and Jonathan T Barron. Nerf in the dark: High dynamic range view synthesis from noisy raw images. In *CVPR*, 2022.
- [28] Ben Mildenhall, Pratul P Srinivasan, Matthew Tancik, Jonathan T Barron, Ravi Ramamoorthi, and Ren Ng. Nerf: Representing scenes as neural radiance fields for view synthesis. In *ECCV*, 2020.
- [29] Thomas Müller, Alex Evans, Christoph Schied, and Alexander Keller. Instant neural graphics primitives with a multiresolution hash encoding. *SIGGRAPH*, 2022.
- [30] Amal Rannen, Rahaf Aljundi, Matthew B Blaschko, and Tinne Tuytelaars. Encoder based lifelong learning. In *ICCV*, 2017.
- [31] Sylvestre-Alvise Rebuffi, Alexander Kolesnikov, Georg Sperl, and Christoph H Lampert. icarl: Incremental classifier and representation learning. In *CVPR*, 2017.
- [32] Christian Reiser, Songyou Peng, Yiyi Liao, and Andreas Geiger. Kilonerf: Speeding up neural radiance fields with thousands of tiny mlps. In *ICCV*, 2021.
- [33] Anthony Robins. Catastrophic forgetting, rehearsal and pseudorehearsal. *Connection Science*, 1995.
- [34] Barbara Roessle, Jonathan T Barron, Ben Mildenhall, Pratul P Srinivasan, and Matthias Nießner. Dense depth priors for neural radiance fields from sparse input views. In *CVPR*, 2022.
- [35] David Rolnick, Arun Ahuja, Jonathan Schwarz, Timothy Lillicrap, and Gregory Wayne. Experience replay for continual learning. *NeurIPS*, 2019.
- [36] Antoni Rosinol, John J Leonard, and Luca Carlone. Nerf-slam: Real-time dense monocular slam with neural radiance fields. *arXiv preprint arXiv:2210.13641*, 2022.
- [37] Johannes Lutz Schönberger and Jan-Michael Frahm. Structure-from-motion revisited. In *CVPR*, 2016.
- [38] Johannes Lutz Schönberger, Enliang Zheng, Marc Pollefeys, and Jan-Michael Frahm. Pixelwise view selection for unstructured multi-view stereo. In *ECCV*, 2016.
- [39] Hanul Shin, Jung Kwon Lee, Jaehong Kim, and Jiwon Kim. Continual learning with deep generative replay. *NeurIPS*, 2017.
- [40] Julian Straub, Thomas Whelan, Lingni Ma, Yufan Chen, Erik Wijmans, Simon Green, Jakob J Engel, Raul Mur-Artal, Carl Ren, Shobhit Verma, et al. The replica dataset: A digital replica of indoor spaces. *arXiv preprint arXiv:1906.05797*, 2019.
- [41] Edgar Sucar, Shikun Liu, Joseph Ortiz, and Andrew J Davison. imap: Implicit mapping and positioning in real-time. In *ICCV*, 2021.
- [42] Jiaming Sun, Yiming Xie, Linghao Chen, Xiaowei Zhou, and Hujun Bao. Neuralrecon: Real-time coherent 3d reconstruction from monocular video. In *CVPR*, 2021.
- [43] Matthew Tancik, Vincent Casser, Xinchun Yan, Sabeek Pradhan, Ben Mildenhall, Pratul P Srinivasan, Jonathan T Barron, and Henrik Kretschmar. Block-nerf: Scalable large scene neural view synthesis. In *CVPR*, 2022.
- [44] Peng Wang, Lingjie Liu, Yuan Liu, Christian Theobalt, Taku Komura, and Wenping Wang. Neus: Learning neural implicit surfaces by volume rendering for multi-view reconstruction. *NeurIPS*, 2021.
- [45] Qianqian Wang, Zhicheng Wang, Kyle Genova, Pratul P Srinivasan, Howard Zhou, Jonathan T Barron, Ricardo Martin-Brualla, Noah Snavely, and Thomas Funkhouser. Ibrnet: Learning multi-view image-based rendering. In *CVPR*, 2021.
- [46] Yi Wei, Shaohui Liu, Yongming Rao, Wang Zhao, Jiwen Lu, and Jie Zhou. Nerfingmvs: Guided optimization of neural radiance fields for indoor multi-view stereo. In *ICCV*, 2021.
- [47] Ju Xu and Zhanxing Zhu. Reinforced continual learning. *NeurIPS*, 2018.
- [48] Zike Yan, Yuxin Tian, Xuesong Shi, Ping Guo, Peng Wang, and Hongbin Zha. Continual neural mapping: Learning an implicit scene representation from sequential observations. In *ICCV*, 2021.
- [49] Lior Yariv, Jiatao Gu, Yoni Kasten, and Yaron Lipman. Volume rendering of neural implicit surfaces. *NeurIPS*, 2021.
- [50] Lin Yen-Chen, Pete Florence, Jonathan T Barron, Alberto Rodriguez, Phillip Isola, and Tsung-Yi Lin. inerf: Inverting neural radiance fields for pose estimation. In *IROS*, 2021.
- [51] Alex Yu, Ruilong Li, Matthew Tancik, Hao Li, Ren Ng, and Angjoo Kanazawa. Plenotrees for real-time rendering of neural radiance fields. In *ICCV*, 2021.
- [52] Alex Yu, Vickie Ye, Matthew Tancik, and Angjoo Kanazawa. pixelnerf: Neural radiance fields from one or few images. In *CVPR*, 2021.
- [53] Zehao Yu, Songyou Peng, Michael Niemeyer, Torsten Sattler, and Andreas Geiger. Monosdf: Exploring monocular geometric cues for neural implicit surface reconstruction. *NeurIPS*, 2022.

- [54] Kai Zhang, Gernot Riegler, Noah Snaveley, and Vladlen Koltun. Nerf++: Analyzing and improving neural radiance fields. *arXiv preprint arXiv:2010.07492*, 2020.
- [55] Xiaoshuai Zhang, Sai Bi, Kalyan Sunkavalli, Hao Su, and Zexiang Xu. Nerfusion: Fusing radiance fields for large-scale scene reconstruction. In *CVPR*, 2022.
- [56] Na Zhao and Gim Hee Lee. Static-dynamic co-teaching for class-incremental 3d object detection. In *AAAI*, 2022.
- [57] Zihan Zhu, Songyou Peng, Viktor Larsson, Weiwei Xu, Hujun Bao, Zhaopeng Cui, Martin R Oswald, and Marc Pollefeys. Nice-slam: Neural implicit scalable encoding for slam. In *CVPR*, 2022.

Supplementary Material

A Implementation Details

A.1 Method Details

More details about the Random Inquirer. As we explained in the main paper, for the scenes where the camera moves along a trajectory, we randomly generate camera views in the range of each degree of freedom of the camera matrix from the previous data. Specifically, we store the range of six values in the camera matrix, *i.e.*, $r_t = (x_{min}, x_{max}, y_{min}, y_{max}, z_{min}, z_{max}, \alpha_{min}, \alpha_{max}, \beta_{min}, \beta_{max}, \gamma_{min}, \gamma_{max})$, at each time step t . We first randomly choose a time step k from $0 : t - 1$ at time step t , and then randomly generate a group of the six values in the range of r_k to compute the camera matrix.

A.2 Framework Details

Novel View Synthesis. Our network F consists of a density network, a color network, and an uncertainty network. The density network consists of eight fully connected (FC) layers with 256-channel, the color and uncertainty networks are both one FC layer with 128-channel. We train our network with a batch size of 1024 rays, 64 points per ray for the coarse network and $64 + 128$ points per ray for the fine network. We adopt AlexNet [18] to compute LPIPS.

3D Reconstruction. Our network F consists of an SDF network, a color network, and an uncertainty network. The density network consists of eight fully connected (FC) layers with 256-channel, the color and uncertainty networks are both two FC layers with 256-channel. We train our network with a batch size of 1024 rays, each ray samples 96 points.

A.3 Dataset Details

We conduct experiments on four datasets, NeRF-real360 [28], ScanNet [9], Replica [40] and ICL-NUIM [13].

NeRF-real360. We use both two scenes with around 100 images with camera poses in each scene. Following the setting in NeRF [28], we randomly sample 12.5% of images as the test set and use the rest for training. For incremental setting, we split one scene into 10-time steps $\mathcal{D} = \{\mathcal{D}^0, \mathcal{D}^1, \dots, \mathcal{D}^9\}$ in the temporal order.

ScanNet. Following [23], we use scene 101 and scene 241 with > 1000 images at a resolution of 648×484 . We randomly sample 20% of images as the training set and use the rest for testing. The camera poses are optimized by COLMAP [38, 37]. For incremental setting, we split a scene into 10-time steps $\mathcal{D} = \{\mathcal{D}^0, \mathcal{D}^1, \dots, \mathcal{D}^9\}$ in the temporal order.

Replica. Following [53], we use eight scenes from the Replica dataset with 100 images with camera poses in each scene. For incremental setting, we split one scene into 10-time steps $\mathcal{D} = \{\mathcal{D}^0, \mathcal{D}^1, \dots, \mathcal{D}^9\}$ in the temporal order.

ICL-NUIM. We use about 200 images with camera poses and depths. For incremental setting, we split one scene into 10-time steps $\mathcal{D} = \{\mathcal{D}^0, \mathcal{D}^1, \dots, \mathcal{D}^9\}$ in the temporal order.

B Additional Experiments

B.1 More Quantitative Results on Replica

We have included the average quantitative results on the Replica dataset in Tab. 2 of the main paper. For a comprehensive analysis, we further provide the detailed quantitative results for all scenes in Tab. S6. It is evident from the results that our approach outperforms MonoSDF [53] by a significant margin across all scenes and achieves comparable performance to the upper bound batch training method ‘MonoSDF*’.

Table S6: Comparison with baselines on the replica dataset. (Best and second best results are highlighted in bold and underlined, respectively.)

Scene	MonoSDF [53]	MonoSDF* [53]	iMAP [41]	NICE-SLAM [57]	MAS [1]	PackNet [25]	KeyF [17]	Ours
room0	3.94	2.45	4.32	<u>2.80</u>	3.78	4.59	2.83	2.49
room1	6.24	2.97	4.28	<u>2.53</u>	6.24	5.72	2.49	2.54
room2	7.74	2.99	5.10	2.83	6.72	7.29	3.48	<u>2.88</u>
office0	7.96	3.33	5.99	2.14	7.44	6.86	<u>4.11</u>	4.32
office1	11.63	2.77	4.49	2.43	12.78	8.69	4.13	2.85
office2	12.93	3.18	5.19	<u>3.70</u>	11.55	11.42	6.66	3.51
office3	11.09	3.22	4.86	<u>3.67</u>	9.84	7.90	4.37	3.48
office4	7.12	2.64	5.71	<u>3.31</u>	5.47	7.44	3.88	2.81
Average	8.58	2.94	4.99	2.93	7.98	7.49	3.99	<u>3.11</u>

B.2 More Qualitative Results

The results presented in Fig. S6 showcase the 3D reconstruction performances of the baseline ‘MonoSDF’, our proposed approach, and the upper bound batch training method ‘MonoSDF*’. Similarly, Fig. S8 and Fig. S7 demonstrate the novel view synthesis performances of the baseline ‘NeRF’, our proposed approach, and the upper bound batch training method ‘NeRF*’. Through these visualizations, we can conclude that our method consistently addresses the catastrophic forgetting problem and achieves comparable results to the upper bound batch training methods in both the novel view synthesis and 3D reconstruction scenarios.

B.3 Rendered Video

We have included rendered videos on the ScanNet dataset in the ‘ScanNet101.mp4’ and ‘ScanNet241.mp4’ files. In these videos, the term ‘NeRF’ refers to the results obtained from the baseline model, while ‘Ours’ represents the outcomes generated by our proposed model. These videos showcase rendered views from \mathcal{D}^0 to \mathcal{D}^9 . Upon comparing the two, it becomes evident that the baseline model (NeRF [28]) suffers from the catastrophic forgetting problem, leading to low-quality videos with noticeable artifacts such as noise and blur. In contrast, our approach significantly mitigates this problem through the utilization of our proposed teacher-student pipeline, resulting in videos of higher quality and reduced artifacts.

C Limitation

While our method demonstrates a substantial improvement over the baselines in the context of incremental training, there is still room for further enhancement compared to models trained in batch mode. The large-scale nature of the scene provides ample information, and the camera facing-outwards dataset exhibits minimal overlap between views. Consequently, our method may not be able to memorize all the knowledge from the limited images. Even the model trained with batch training can only acquire a limited amount of information about the scene, as illustrated in Fig. S7. Therefore, there is potential for further progress in capturing a more comprehensive understanding of the scene.

D Societal Impacts

Our method excels at faithfully and incrementally reconstructing 3D scenes using limited memory, enabling applications in streaming data scenarios and on small devices. However, it can also have potentially negative social impacts. Firstly, the reconstruction from online streaming data, such as live broadcasts, may raise privacy concerns that require careful consideration and appropriate safeguards. Additionally, the accessibility of scene reconstruction capabilities on small devices may increase the risk of their misuse for illegal applications.

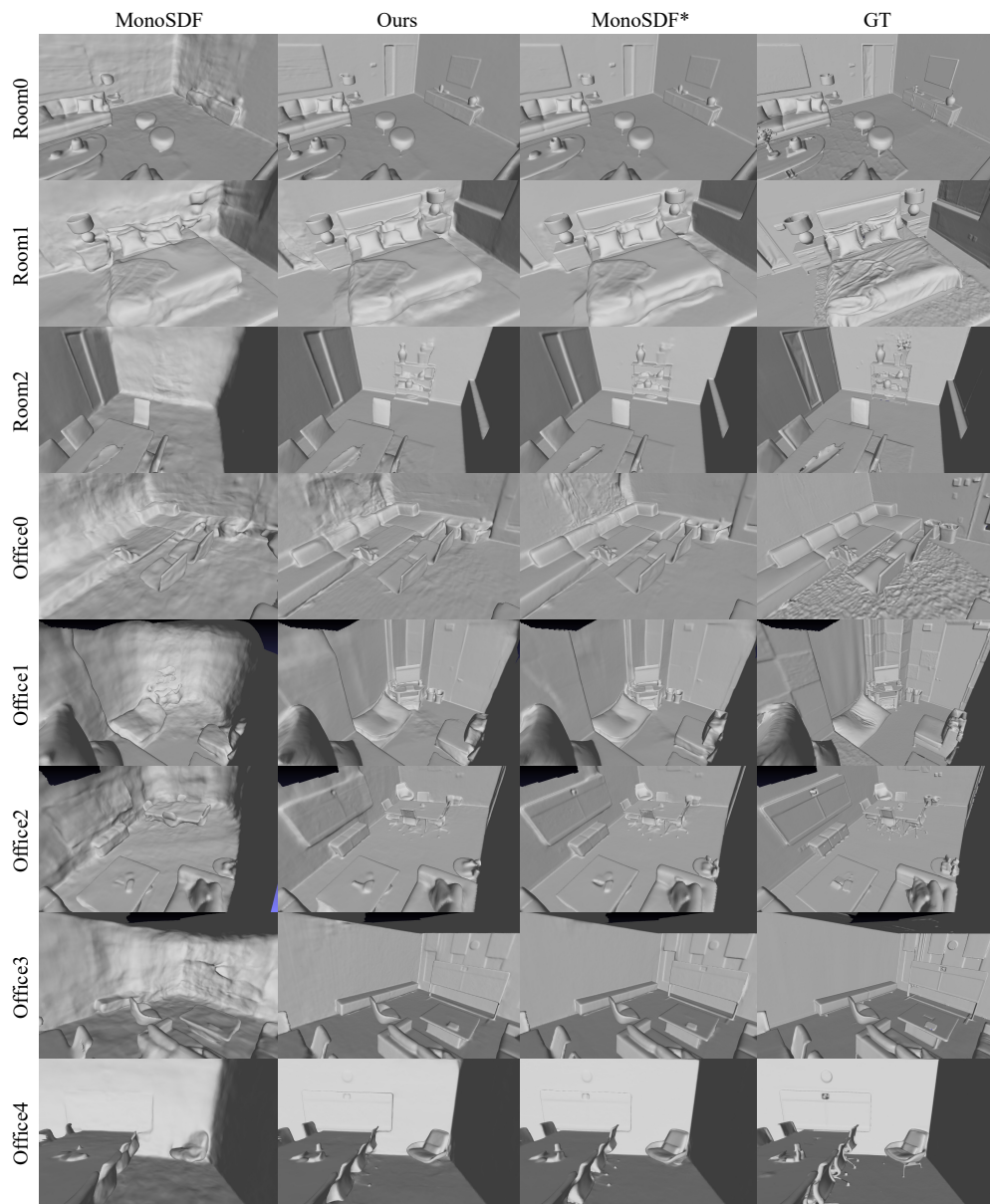


Figure S6: Qualitative comparison with the baseline ‘MonoSDF’ and upper bound batch training method ‘MonoSDF*’ on eight scenes of the Replica dataset. ‘GT’ represents the ground truth images. ‘MonoSDF’ and ‘Ours’ models are incrementally trained on the 10-step training datasets.

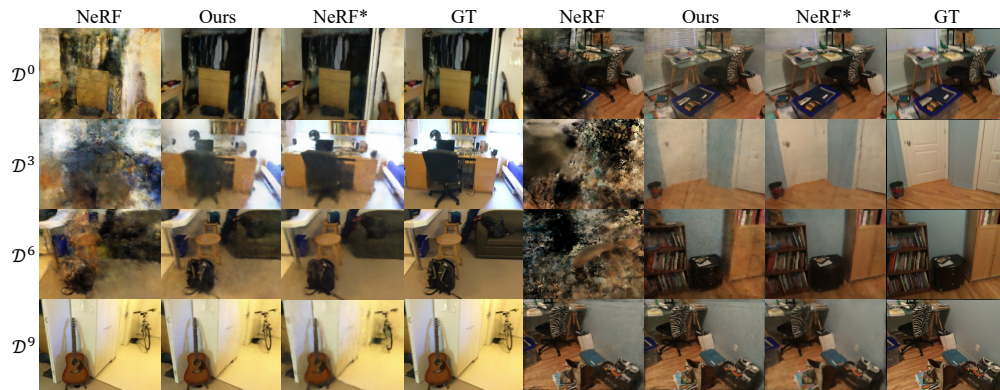


Figure S7: Qualitative comparison with the baseline ‘NeRF’ and upper bound batch training method ‘NeRF*’ on scene 101 (left) and 241 (right) of ScanNet dataset. ‘GT’ represents the ground truth images and $\mathcal{D}^0, \mathcal{D}^3, \mathcal{D}^6, \mathcal{D}^9$ denote the results from each time step test views. ‘NeRF’ and ‘Ours’ models are incrementally trained on the 10-step training datasets.

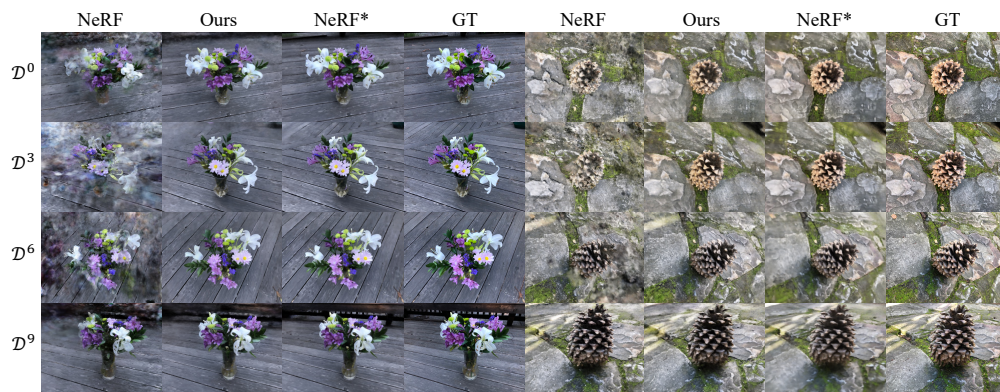


Figure S8: Qualitative comparison with the baseline ‘NeRF’ and upper bound batch training method ‘NeRF*’ on scene *Vasdeck* (left) and *Pinecone* (right) of NeRF-real360 dataset. ‘GT’ represents the ground truth images and $\mathcal{D}^0, \mathcal{D}^3, \mathcal{D}^6, \mathcal{D}^9$ denote the results from each time step test views. ‘NeRF’ and ‘Ours’ models are incrementally trained on the 10-step training datasets.